European Journal of Nuclear Medicine and Molecular Imaging
https://doi.org/10.1007/s00259-018-4125-x

ORIGINAL ARTICLE

# Differences in gray and white matter $^{18}$F-THK5351 uptake between behavioral-variant frontotemporal dementia and other dementias

Hye Joo Son[1] · Jungsu S. Oh[1] · Jee Hoon Roh[2] · Sang Won Seo[3] · Minyoung Oh[1] · Sang Ju Lee[1] · Seung Jun Oh[1] · Jae Seung Kim[1]

Received: 25 March 2018 / Accepted: 3 August 2018


## Abstract

**Purpose** We investigated the regional distribution of $^{18}$F-THK5351 uptake in gray (GM) and white matter (WM) in patients with behavioral-variant frontotemporal dementia (bvFTD) and compared it with that in patients with Alzheimer's disease (AD) or semantic dementia (SD).

**Methods** $^{18}$F-THK-5351 positron emission tomography (PET), $^{18}$F-florbetaben PET, magnetic resonance imaging, and neuropsychological testing were performed in 103 subjects including 30, 24, 9, and 8 patients with mild cognitive impairment, AD, bvFTD, and SD, respectively, and 32 normal subjects. Standardized uptake value ratios (SUVRs) of $^{18}$F-THK-5351 PET images were measured from six GM and WM regions using cerebellar GM as reference. GM and WM SUVRs and WM/GM ratios, the relationship between GM SUVR and WM/GM ratio, and correlation between SUVR and cognitive function were compared.

**Results** In AD, both parietal GM ($p < 0.001$) and WM ($p < 0.001$) SUVRs were higher than in bvFTD. In AD and SD, the WM/GM ratio decreased as the GM SUVR increased, regardless of lobar region. In AD, memory function correlated with parietal GM ($\rho = -0.74$, $p < 0.001$) and WM ($\rho = -0.53$, $p < 0.001$) SUVR. In SD, language function correlated with temporal GM SUVR ($\rho = -0.69$, $p = 0.006$). The frontal WM SUVR was higher in bvFTD than in AD ($p = 0.003$) or SD ($p = 0.017$). The frontal WM/GM ratio was higher in bvFTD than in AD ($p < 0.001$). In bvFTD, the WM/GM ratio increased more prominently than the GM SUVR only in the frontal lobe ($R^2 = 0.026$). In bvFTD, executive function correlated with frontal WM SUVR ($\rho = -0.64$, $p = 0.014$).

**Conclusions** Frontal WM $^{18}$F-THK5351 uptake was higher in bvFTD than in other dementias. The increase in frontal WM uptake was greater than the increase in GM uptake and correlated with executive function. This suggests that frontal lobe WM $^{18}$F-THK5351 uptake reflects neuropathological differences between bvFTD and other dementias.

**Keywords** Behavioral-variant frontotemporal dementia · $^{18}$F-THK-5351 · PET · White matter · Tau

Hye Joo Son and Jungsu S. Oh contributed equally to this work.

**Electronic supplementary material** The online version of this article (https://doi.org/10.1007/s00259-018-4125-x) contains supplementary material, which is available to authorized users.

✉ Jae Seung Kim
jaeskim@amc.seoul.kr

[1] Department of Nuclear Medicine, Asan Medical Center, University of Ulsan College of Medicine, 88 Olympic-ro 43-gil, Songpa-gu, Seoul 05505, Republic of Korea

[2] Department of Neurology, Asan Medical Center, University of Ulsan College of Medicine, 88 Olympic-ro 43-gil, Songpa-gu, Seoul 05505, Republic of Korea

[3] Department of Neurology, Samsung Medical Center, Sungkyunkwan University School of Medicine, 81 Irwon-Ro Gangnam-gu, Seoul 06351, Republic of Korea

Published online: 14 August 2018

## Introduction

Tauopathies comprise several neurodegenerative dementias characterized by tau aggregation in neuronal and glial cells [1]. One member of this group, behavioral-variant frontotemporal dementia (bvFTD), is a clinical syndrome characterized by progressive changes in social interaction [2], and is often mistaken for Alzheimer's disease (AD) because of overlapping symptoms [3]. Frontal-variant AD often mimics bvFTD; 10–40% of patients with bvFTD have been found to exhibit AD pathology [4–6].

Although most tauopathies involve gray matter (GM), recent evidence highlights the significance of white matter (WM) in evaluating patients with bvFTD. A study using magnetic resonance imaging (MRI) reported abnormal signal intensities in the frontal WM of patients with bvFTD [7]. A histological study demonstrated that AD and bvFTD were notable for distinct neuroinflammation distribution between GM and WM, with bvFTD exhibiting prominent microglial activation in the frontal and temporal WM, whereas no differences in GM and WM were found in AD [8].

Microglia-driven neuroinflammation may accelerate neurodegeneration by contributing to the spread of tau-containing neurofibrillary tangles [9, 10]. Recent developments in tau-selective radiotracers, such as $^{18}$F-AV-1451, have enabled the investigation of differences in tau pathology between GM and WM among various tauopathies [11]. While tau binding is observed mainly in GM in AD, non-AD tauopathies are characterized by tau binding in subcortical WM and GM [11].

The novel tau PET tracer $^{18}$F-THK5351 is a single S-enantiomer quinoline-derivative probe exhibiting high affinity to tau neurofibrillary tangles [12]. A substantial reduction in $^{18}$F-THK5351 uptake was reported after administration of the monoamine oxidase B (MAO-B) inhibitor selegiline [13]. Considering the role of neuroinflammation in the propagation of neurodegeneration, $^{18}$F-THK5351 PET may reflect the mixed pathology of tau and astrocytosis in dementia [13, 14]. In this work, we investigated the regional distribution of $^{18}$F-THK5351 uptake in GM and WM of patients with bvFTD and compared it with that in patients with AD or semantic dementia (SD). Based on previous pathological evidence, our a priori hypothesis was that $^{18}$F-THK5351 uptake in frontal WM would be higher in patients with bvFTD than in those with other dementias.

## Materials and methods

### Subjects

Two hundred twenty subjects, including those on the AD spectrum [mild cognitive impairment (MCI) and AD], those with non-AD tauopathies (bvFTD and SD), and controls, were enrolled prospectively. Subjects were recruited from the MEMORI cohorts at Asan Medical Center and Samsung Medical Center between January 2016 and August 2017. All subjects underwent brain MRI and two rounds of PET with $^{18}$F-THK5351 for tau and $^{18}$F-florbetaben for amyloid-β (Aβ) as well as neuropsychological testing. Overall, 103 subjects were selected based on Aβ positivity: Aβ-positive MCI ($n$ = 30; mean age, 69.7 ± 6.9 years), Aβ-positive AD ($n$ = 24; mean age, 62.7 ± 10.6 years), Aβ-negative bvFTD ($n$ = 9; mean age, 64.3 ± 9.8 years), Aβ-negative SD ($n$ = 8; mean age, 63.4 ± 6.4 years), and Aβ-negative healthy controls ($n$ = 32; mean age, 69.3 ± 6.0 years).

All subjects completed the Seoul Neuropsychological Screening Battery, which assesses attention, visuospatial function, language, memory, and executive function, as well as the Korean version of the Mini-Mental State Examination (K-MMSE) [15]. Scores below the 16th percentile (one standard deviation) compared with sex-, age-, and education-specific norms were regarded as abnormal. Patients with AD met the criteria recommended by the National Institute on Aging-Alzheimer's Association [16], and patients with MCI met the Petersen criteria [17]. Patients with bvFTD met the criteria for FTD proposed by Knopman et al. [18] and were classified as bvFTD or SD. This study was approved by the Asan Medical Center and Samsung Medical Center Institutional Review Board for Human Research. Written informed consent was obtained from all subjects (ClinicalTrials.gov identifier NCT02656498).

### Acquisition of PET and MRI images

All PET images were acquired using Discovery 690, 710, and 690 Elite PET/CT scanners (GE Healthcare; Milwaukee, WI, USA) at Asan Medical Center and a Discovery STE PET/CT scanner (GE Healthcare) at Samsung Medical Center with the same imaging/reconstruction protocols. Tau PET images were obtained for 20 min, beginning 50 min after injection of 185 ± 18.5 MBq of $^{18}$F-THK5351. Amyloid PET images were obtained for 20 min, beginning 90 min after injection of 300 ± 30 MBq of $^{18}$F-florbetaben. Three-dimensional volumetric T1-weighted MRI scans were acquired to create cortical volumes of interest (VOIs) for both quantification and partial volume correction of PET images. Refer to the Appendix in the supplementary material for further details.

### Image processing

Each subject's PET image was rigidly co-registered to their magnetization-prepared rapid gradient-echo data using the SPM8 [Statistical Parametric Mapping] tool (Wellcome Trust Centre for Neuroimaging, Institute of Neurology, University College London) in MATLAB R2013a software for Windows (The MathWorks, Natick, MA, USA). As described by Thomas

et al. [19], cortical GM/WM parcellation was performed using Freesurfer 5.3 software (Massachusetts General Hospital, Harvard Medical School, http://surfer.nmr.mgh.harvard.edu); this gyral parcellation is based on the Desikan-Killiany atlas for both quantification and partial volume effect (PVE) correction of PET images. Region-based PVE correction was performed using the geometric transfer matrix approach. Voxel-based PVE correction was carried out using the ratio of region-based partial volume effect (PVE)-corrected PET to its 7-mm-smoothed image. Subcortical WM regions were segmented using cortical labels overlaid on the WM surface with voxels within a 5-mm depth from the GM boundary. By merging anatomically related regions, participant-specific VOI mask images were created for six GM regions (frontal, temporal, parietal, and occipital lobes, and central and cingulate gyri) and corresponding WM regions. The mean standardized uptake value ratio (SUVR) was calculated for each VOI based on the mean SUV for each VOI and normalized to the mean SUV of cerebellar GM. The main outcome measures were the mean SUVR for each GM (SUVR [GM]) and WM (SUVR [WM]), the WM/GM ratio, and the percentage of normal WM/GM ratio. The percentage of normal WM/GM ratio was calculated by dividing the WM/GM ratio of each subject by the mean WM/GM ratio of the controls.

### Statistics

Demographic data were compared using Kruskal–Wallis, chi-squared, or Fisher's exact tests. Group comparisons for GM and WM $^{18}$F-THK5351 uptake were performed by comparing SUVRs, WM/GM ratios, and percentages of normal WM/GM ratio among bvFTD, AD, and SD patients. Parametrically distributed data were analyzed using analysis of variance for between-group comparisons and the Student *t* test for comparisons between pairs of groups. The Bonferroni correction was applied to the post hoc analyses of the within-group comparisons to correct for the number of comparisons performed (two comparisons for each variable: bvFTD vs. AD and bvFTD vs. SD). Spearman's correlation was used to evaluate the relationship between SUVRs and cognitive function. For Bonferroni-corrected tests, $p$ values $< 0.025$ were considered statistically significant. In other tests, $p < 0.05$ was considered statistically significant. SPSS for Windows version 18.0 (SPSS Inc., Chicago, IL, USA) was used for all statistical analyses. Data for study variables are expressed as means ± standard deviation.

## Results

### Demographic characteristics

There were no differences in sex, disease duration, or years of education among the groups (Table 1). Healthy controls and MCI patients were older than bvFTD, AD, and SD patients ($p = 0.02$). There were no difference in age, sex, disease duration, years of education, K-MMSE scores, or clinical dementia rating scores among patients with AD, bvFTD, and SD.

### Distribution of GM and WM $^{18}$F-THK5351 uptake

Representative $^{18}$F-THK5351 PET images of control, AD, SD, and bvFTD patients are shown (Fig. 1). In GM, patients with AD had the highest GM SUVRs in the frontal, parietal, and occipital lobes and the central and cingulate gyri. This effect was most pronounced in the parietal lobe (AD, 2.50 ± 0.74; control, 1.63 ± 0.32; $p < 0.001$; Fig. 2a).

Patients with SD had the highest GM SUVRs in the temporal lobe (SD, 2.44 ± 0.68; control, 1.76 ± 0.20; $p < 0.001$; Fig. 2a). In WM, patients with bvFTD had the highest WM SUVRs in the frontal lobe (bvFTD, 1.66 ± 0.60; control, 1.09 ± 0.16; $p < 0.001$; Fig. 2b).

### Group comparisons of GM and WM $^{18}$F-THK5351 uptake

Table 2 shows the SUVRs for GM and WM as well as the WM/GM ratio for each group. GM SUVRs in the parietal lobe were higher in AD (2.50 ± 0.74) than in bvFTD (1.65 ± 0.15; $p < 0.001$). WM SUVRs in the parietal lobe were higher in AD (1.40 ± 0.25) than in bvFTD (1.15 ± 0.12; $p < 0.001$). WM SUVRs in the frontal lobe were higher in bvFTD (1.66 ± 0.60) than in AD (1.34 ± 0.22; $p = 0.003$) and SD (1.23 ± 0.29; $p = 0.017$), although there were no differences in frontal lobe GM SUVRs between bvFTD and AD. The WM/GM ratio in the frontal lobe was higher in bvFTD (0.85 ± 0.26) than in AD (0.67 ± 0.10; $p < 0.001$) and SD (0.70 ± 0.14; $p = 0.04$). Detailed results of PVE-uncorrected images are presented as supplemental data.

We examined sensitivity, specificity, and diagnostic accuracy to determine the differential diagnosis between FTD and non-FTD (AD and SD) with respect to the GM SUVR, WM SUVR, and WM/GM ratios of the frontal, temporal, and parietal lobes, the areas in which the target lesions were located (Table 3). The frontal WM SUVR and frontal WM/GM ratios showed the highest accuracy in both PVE-corrected (frontal WM/GM ratio AUC: 0.71) and PVE-uncorrected (frontal WM SUVR AUC: 0.70, frontal WM/GM ratio AUC: 0.73) images.

### Comparison of the relationship between GM SUVR and WM/GM ratio

In AD and SD, the WM/GM ratio decreased with increasing GM SUVR in the frontal, temporal, and parietal lobes (Fig. 3). Conversely, in bvFTD, the WM/GM ratio increased more prominently than the GM uptake only in the frontal lobe

**Table 1** Characteristics of the study population

| | Control ($n = 32$) | MCI ($n = 30$) | AD ($n = 24$) | bvFTD ($n = 9$) | SD ($n = 8$) | $p$ value (all groups) | $p$ value (bvFTD vs. AD vs. SD) |
|---|---|---|---|---|---|---|---|
| Age (years) | 69.3 ± 6 | 69.7 ± 6.9 | 62.7 ± 10.6 | 64.3 ± 9.8 | 63.4 ± 6.4 | 0.02 | 0.96 |
| Sex (M/F) | 12/20 | 10/19 | 12/12 | 4/4 | 5/3 | 0.14 | 0.82 |
| Disease duration (years) | 3.3 ± 2.6 | 3.4 ± 2.7 | 3.7 ± 2.8 | 5.1 ± 8.4 | 4.5 ± 3.1 | 0.82 | 0.57 |
| Education (years) | 10.4 ± 4.8 | 11.1 ± 4.2 | 11.5 ± 4.4 | 11.6 ± 4.1 | 11.8 ± 2.6 | 0.82 | 0.82 |
| K-MMSE total score | 28.5 ± 1.2 | 24.5 ± 3.7 | 20.7 ± 5.6 | 19.9 ± 2.6 | 21.1 ± 9 | <0.001 | 0.41 |
| K-MMSE z score | 0.3 ± 0.9 | −1.9 ± 1.9 | −5.5 ± 4.5 | −6 ± 2.5 | −5 ± 5.6 | <0.001 | 0.71 |
| CDR score | 0.2 ± 0.2 | 0.5 ± 0.1 | 0.9 ± 0.6 | 1.3 ± 0.7 | 0.8 ± 0.5 | <0.001 | 0.23 |
| GDS score | 2 ± 0.4 | 3.1 ± 0.5 | 4.1 ± 0.8 | 4.7 ± 0.8 | 3.5 ± 0.5 | <0.001 | 0.04 |
| Z score for SNSB attention subdomain | 0.5 ± 1 | −0.2 ± 0.9 | −0.7 ± 1.2 | −1.2 ± 0.8 | −1.1 ± 2.1 | <0.001 | 0.66 |
| Z score for SNSB language subdomain | 1 ± 1.1 | −1.6 ± 2.9 | −2.5 ± 3 | −5.1 ± 4.1 | −8.4 ± 7.4 | <0.001 | 0.13 |
| Z score for SNSB visuospatial subdomain | 0.3 ± 0.9 | −0.8 ± 1.4 | −7 ± 6.2 | −4.6 ± 2.6 | −2.2 ± 2.5 | <0.001 | 0.16 |
| Z score for SNSB memory subdomain | 0.7 ± 0.7 | −2.3 ± 1.2 | −3.5 ± 1.8 | −3.6 ± 1.3 | −3.1 ± 1.1 | <0.001 | 0.89 |
| Z score for SNSB executive subdomain | 0.5 ± 1 | −1.6 ± 1.7 | −4.6 ± 3.7 | −5.8 ± 2.5 | −2 ± 2.2 | <0.001 | 0.11 |

*MCI* mild cognitive impairment, *AD* Alzheimer's disease, *bvFTD* behavioral-variant frontotemporal dementia, *SD* semantic dementia, *MMSE* Mini-Mental State Examination, *CDR* Clinical Dementia Rating, *GDS* Global Deterioration Scale, *SNSB* Seoul Neuropsychological Screening Battery

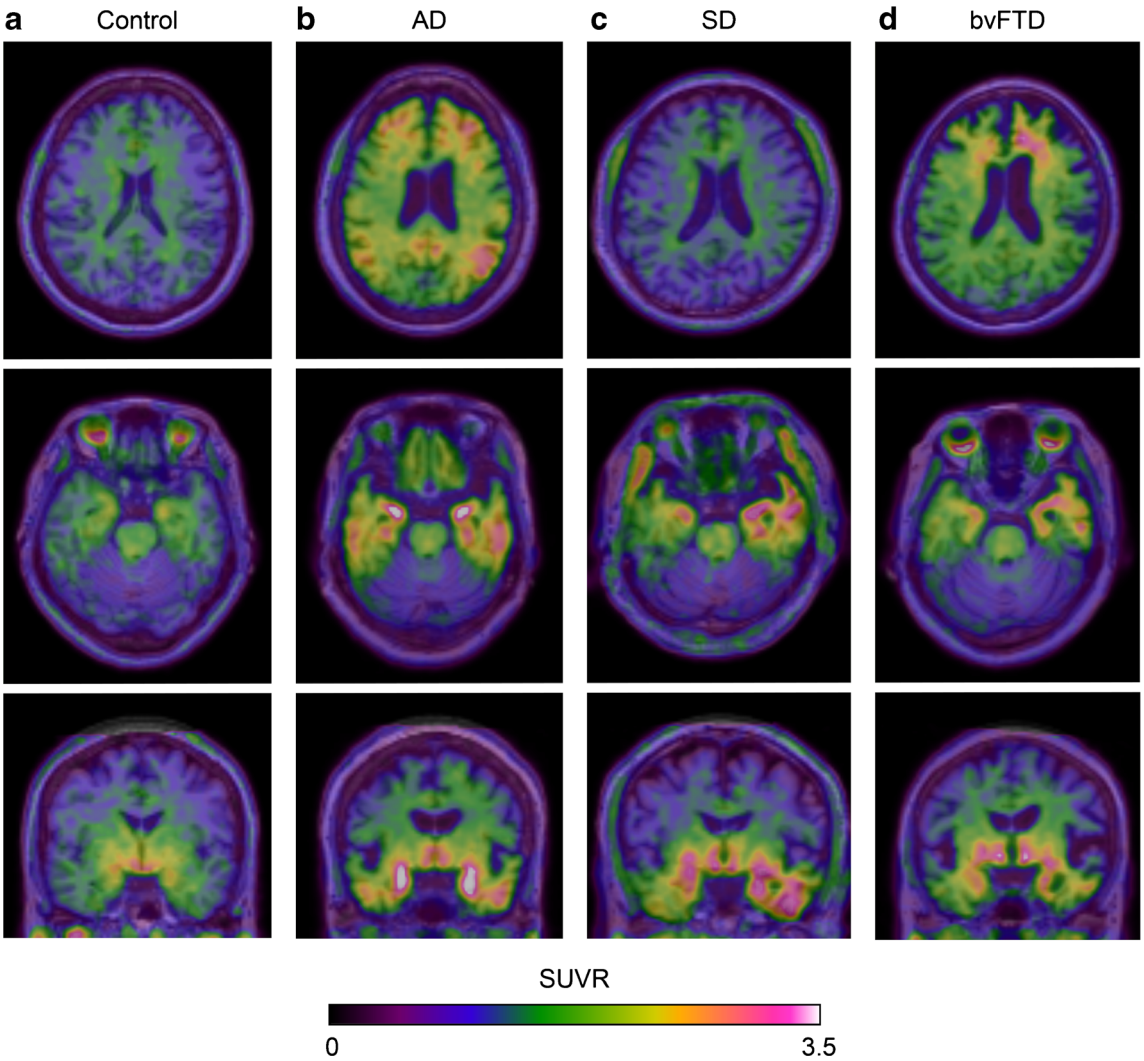


**Fig. 1** Representative $^{18}$F-THK5351 positron emission tomography images of normal controls (**a**) and patients with AD (**b**), SD (**c**), and bvFTD (**d**)

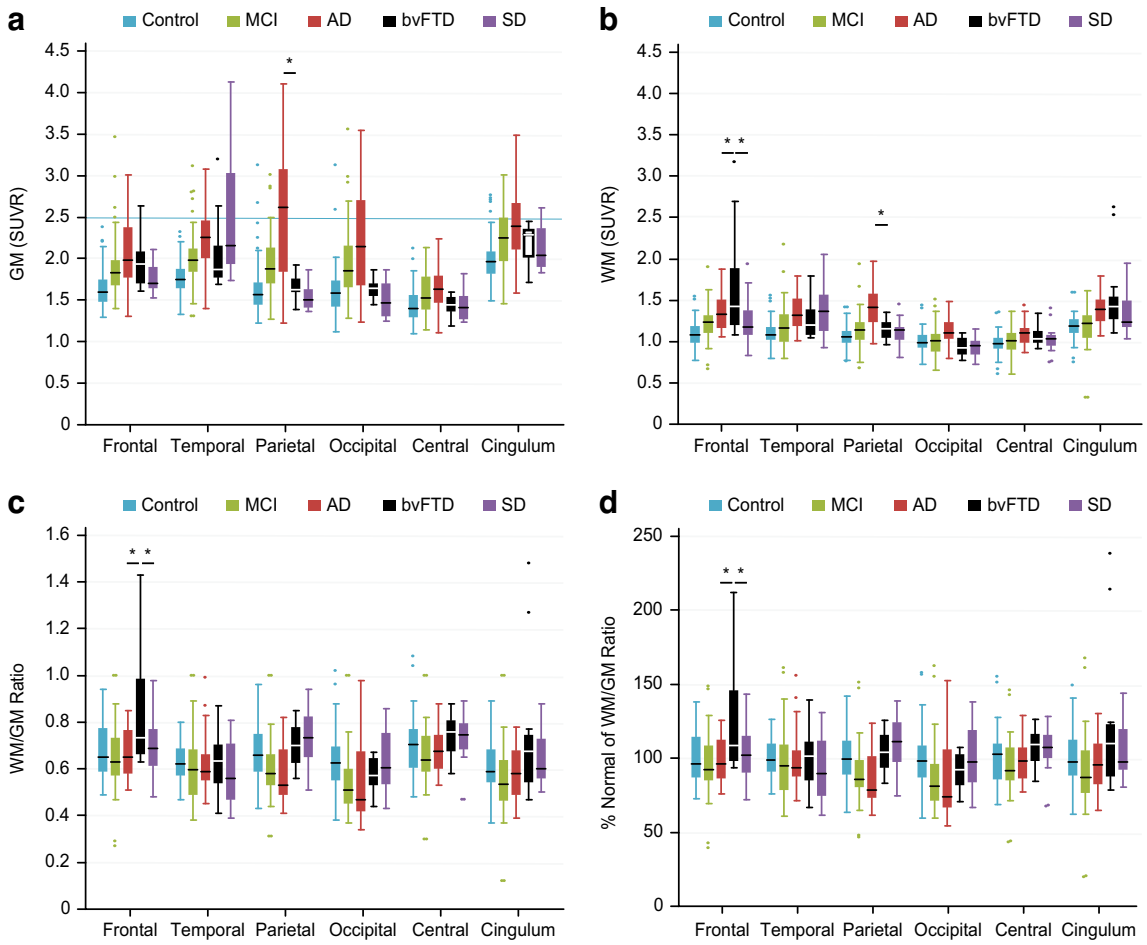


**Fig. 2** SUVR of GM (**a**) and WM (**b**), WM/GM ratio (**c**), and percentage normal WM/GM ratio (**d**). Statistical significance for each comparison is shown at the top of each plot

**Table 2** Group comparisons of GM and WM $^{18}$F-THK5351 uptake

| | | bvFTD | | AD | | SD | | *p* value | bvFTD vs. AD | bvFTD vs. SD |
|---|---|---|---|---|---|---|---|---|---|---|
| GM (SUVR) | Frontal | 1.93 | [0.28] | 2.05 | [0.40] | 1.76 | [0.19] | 0.02 | 0.27 | 0.05 |
| | Temporal | 2.04 | [0.40] | 2.24 | [0.39] | 2.44 | [0.68] | 0.06 | 0.08 | 0.05 |
| | Parietal | 1.65 | [0.15] | 2.50 | [0.74] | 1.54 | [0.15] | <.001 | <.001 | 0.04 |
| | Occipital | 1.64 | [0.11] | 2.22 | [0.62] | 1.50 | [0.20] | <.001 | <.001 | 0.03 |
| | Central | 1.44 | [0.12] | 1.62 | [0.25] | 1.43 | [0.17] | 0.001 | 0.006 | 0.91 |
| | Cingulum | 2.18 | [0.22] | 2.43 | [0.43] | 2.12 | [0.26] | 0.005 | 0.03 | 0.51 |
| WM (SUVR) | Frontal | 1.66 | [0.60] | 1.34 | [0.22] | 1.23 | [0.29] | 0.002 | 0.003 | 0.017 |
| | Temporal | 1.25 | [0.21] | 1.35 | [0.23] | 1.37 | [0.30] | 0.29 | 0.11 | 0.22 |
| | Parietal | 1.15 | [0.12] | 1.40 | [0.25] | 1.12 | [0.17] | <.001 | <.001 | 0.55 |
| | Occipital | 0.94 | [0.11] | 1.12 | [0.16] | 0.93 | [0.12] | <.001 | <.001 | 0.92 |
| | Central | 1.06 | [0.11] | 1.09 | [0.14] | 1.03 | [0.17] | 0.29 | 0.42 | 0.54 |
| | Cingulum | 1.53 | [0.44] | 1.39 | [0.19] | 1.35 | [0.26] | 0.13 | 0.08 | 0.17 |
| WM/GM ratio | Frontal | 0.85 | [0.26] | 0.67 | [0.10] | 0.70 | [0.14] | <.001 | <.001 | 0.04 |
| | Temporal | 0.63 | [0.13] | 0.61 | [0.11] | 0.58 | [0.14] | 0.49 | 0.64 | 0.32 |
| | Parietal | 1.93 | [0.28] | 2.05 | [0.40] | 1.76 | [0.19] | 0.02 | 0.27 | 0.05 |
| | Occipital | 2.04 | [0.40] | 2.24 | [0.39] | 2.44 | [0.68] | 0.06 | 0.08 | 0.05 |
| | Central | 1.65 | [0.15] | 2.50 | [0.74] | 1.54 | [0.15] | <.001 | <.001 | 0.04 |
| | Cingulum | 1.64 | [0.11] | 2.22 | [0.62] | 1.50 | [0.20] | <.001 | <.001 | 0.03 |

*bvFTD* behavioral-variant frontotemporal dementia, *AD* Alzheimer's disease, *SD* semantic dementia, *SUVR*, standardized uptake value ratio, *GM* gray matter, *WM* white matter

**Table 3** Receiver operating characteristic (ROC) curve analysis for distinguishing FTD from non-FTD

| | | PVE-uncorrected Accuracy (AUC) | PVE- corrected Accuracy (AUC) | PVE- uncorrected Cut-off value | PVE- corrected Cut-off value | PVE- uncorrected Sensitivity | PVE- corrected Sensitivity | PVE- uncorrected Specificity | PVE- corrected Specificity |
|---|---|---|---|---|---|---|---|---|---|
| GM (SUVR) | Frontal | 0.36 | 0.51 | 1.31 | 2.12 | 0.72 | 0.31 | 0.25 | 1.00 |
| | Temporal | 0.65 | 0.68 | 1.55 | 1.87 | 0.66 | 0.84 | 0.75 | 0.63 |
| | Parietal | 0.67 | 0.70 | 1.49 | 2.00 | 0.53 | 0.53 | 1.00 | 1.00 |
| WM (SUVR) | Frontal | 0.70 | 0.66 | 2.07 | 1.81 | 0.38 | 0.38 | 1.00 | 0.97 |
| | Temporal | 0.64 | 0.59 | 1.80 | 1.48 | 0.47 | 0.28 | 0.88 | 1.00 |
| | Parietal | 0.67 | 0.71 | 1.65 | 1.33 | 0.50 | 0.50 | 1.00 | 1.00 |
| WM/GM ratio | Frontal | 0.73 | 0.71 | 1.29 | 0.62 | 0.50 | 1.00 | 0.97 | 0.44 |
| | Temporal | 0.53 | 0.57 | 1.15 | 0.58 | 0.38 | 0.75 | 0.81 | 0.56 |
| | Parietal | 0.58 | 0.70 | 1.10 | 0.54 | 1.00 | 1.00 | 0.34 | 0.47 |

*PVE* partial volume effect, *GM* gray matter, *WM* white matter

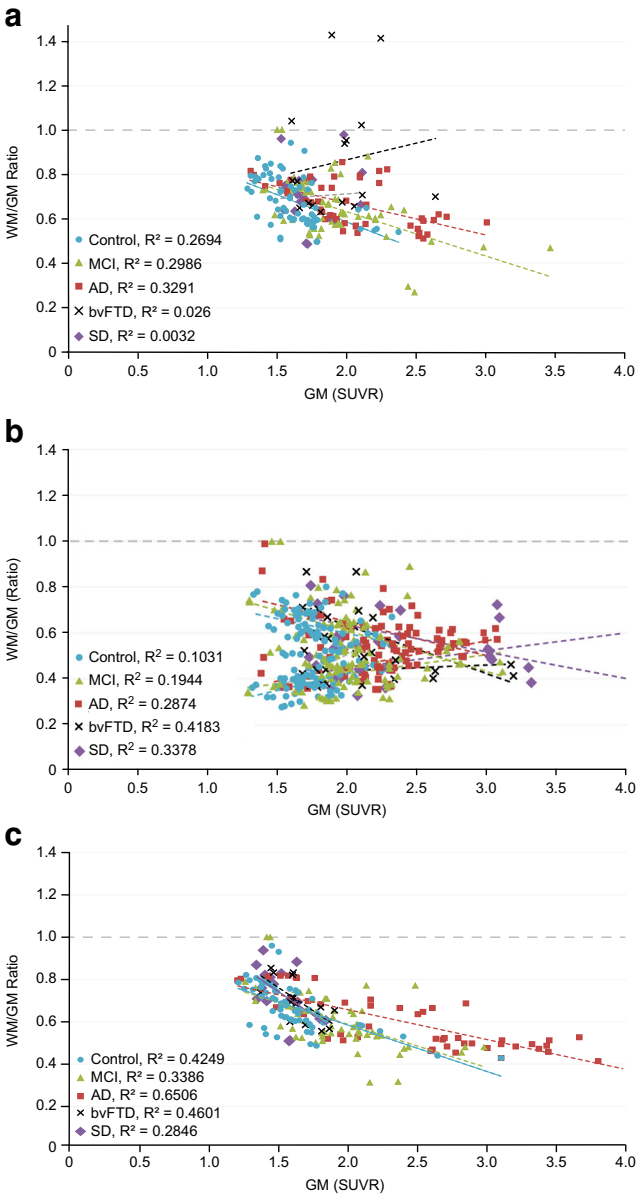


**Fig. 3** Relations between WM/GM ratio and GM SUVR in the frontal (**a**), temporal (**b**), and parietal (**c**) lobes

($R^2 = 0.026$; Fig. 3a). In the temporal lobe, the WM/GM ratio decreased ($R^2 = 0.418$) as the GM SUVR increased (Fig. 3b). In the parietal lobes of patients with bvFTD, both the WM and the GM uptake were similar to those in healthy controls (Fig. 3c).

## Correlation between $^{18}$F-THK5351 uptake and cognitive function

In AD, both the GM (Spearman's $\rho = -0.79$, $p < 0.001$) and WM (Spearman's $\rho = -0.59$, $p < 0.001$) SUVRs of the parietal lobe correlated with K-MMSE scores. Additionally, both GM (Spearman's $\rho = -0.74$, $p < 0.001$) and WM (Spearman's $\rho = -0.53$, $p < 0.001$) SUVRs of the parietal lobe correlated with

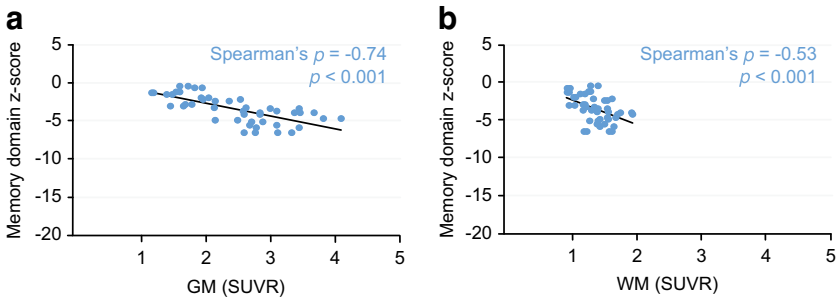


**Fig. 4** **a** Correlations between GM SUVR of the parietal lobe and memory function in AD. **b** Correlations between WM SUVR of the parietal lobe and memory function in AD

memory function (Fig. 4a, b). In the WM but not the GM of patients with bvFTD, the SUVR (Spearman's $\rho = -0.64$, $p = 0.014$) of the frontal lobe correlated with executive function (Fig. 5a). Conversely, in the GM but not WM of patients with SD, the SUVR (Spearman's $\rho = -0.69$, $p = 0.006$) of the temporal lobe correlated with language function (Fig. 5b).

## Discussion

Tau PET has been used in previous research to visualize tau pathology distribution and monitor disease progression [20]. In the present study, frontal $^{18}$F-THK5351 uptake was higher in bvFTD than in other dementias only in the WM, and correlated with executive function in bvFTD. This is the first report to show that the relative distribution of $^{18}$F-THK5351 uptake between GM and WM in a certain lobar area differs according to neuropathology.

The increased $^{18}$F-THK5351 uptake in the frontal WM is consistent with the vulnerability of this region to bvFTD pathology. Tau pathology in bvFTD in frontal WM is observed as neuropil threads and oligodendroglial coiled bodies [21, 22]. An immunohistochemistry study showed that increased tau binding was dominant in GM in AD, with global GM/WM ratios of 2–4 [11]. However, in bvFTD, tau binding was observed in WM as well as GM, with lower GM/WM ratios than those observed in AD [11]. In postmortem brain tissue from a patient with bvFTD, activated microglia in the frontal WM were found to be tau-immunoreactive [21]. Higher microglial activation in patients with bvFTD versus AD is demonstrated only in the frontal WM [10]. Neuroinflammatory factors increase throughout the disease course and correlate positively with tau burden, contributing to neurodegeneration [14, 23]. The $^{18}$F-THK5351 PET signal was reported to reflect tau immunoreactivity and activated glial cells, and is useful in the assessment of tau-associated neuroinflammatory changes [14].

In MR-diffusion tensor imaging (DTI) studies, compared with AD, bvFTD was associated with a greater decrease in fractional anisotropy in the frontal WM [24, 25]. In our patients with bvFTD, WM uptake increased more prominently than GM uptake only in the frontal lobe. Because neurodegeneration starts with GM loss, increased GM uptake correlates with disease progression. It still unknown whether WM degeneration is a primary step independent of GM deterioration, or an outcome of Wallerian degeneration propagated from nearby GM damage [26, 27]. Previous MRI studies comparing WM changes to regional GM atrophy in bvFTD demonstrated that WM microstructural damage in the anterior corpus callosum and cingulate gyrus spatially exceeded GM volume loss [24, 28]. These findings constitute indirect and direct evidence of WM pathology in bvFTD.

Notably, in bvFTD, WM uptake did not increase in proportion to the increase in GM uptake in the temporal lobe, as was observed in AD. Off-target MAO-B binding or the effects of normal aging in the entorhinal cortex may contribute to high $^{18}$F-THK5351 uptake in temporal GM [29]. An MR-DTI study reported that WM changes in the uncinate fasciculus were co-localized with GM atrophy of the anterior temporal lobe [24]. Whether $^{18}$F-THK5351 uptake in the parietal and frontal regions—sites of pathological lesions in AD and bvFTD, respectively—reflects inherent pathological or lobar-specific anatomical characteristics remains unclear. In the present study, similar GM and WM relationships were observed in the temporal lobe, a common site for AD and

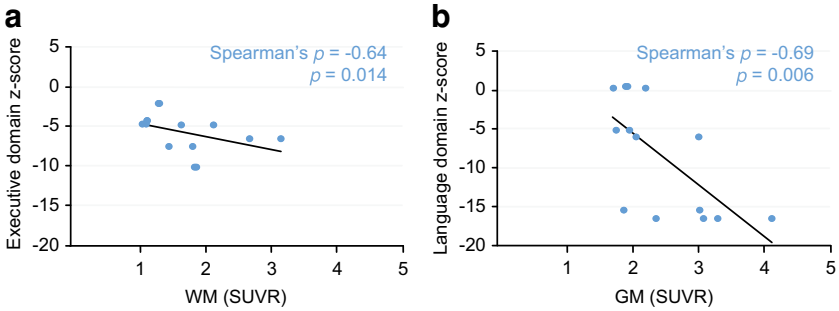


**Fig. 5** **a** Correlations between WM SUVR of the frontal lobe and executive function in bvFTD. **b** Correlations between GM SUVR of the temporal lobe and language function in SD

bvFTD pathology, in patients with AD and bvFTD, possibly because of lobar-specific anatomical characteristics.

Within the spectrum of frontotemporal lobar degeneration, the semantic variant of primary progressive aphasia (svPPA or SD) displays TAR DNA-binding protein 43 (TDP-43) pathology in 75–90% of cases (svPPA-TDP), with tau pathology (svPPA-tau) infrequently present at postmortem examination [30, 31]. Conversely, bvFTD displays either TDP-43 or tau pathology with nearly equal likelihood [32]. Although an increase in $^{18}$F-THK5351 uptake is not expected in SD with TDP-43 pathology, our patients with SD exhibited prominent $^{18}$F-THK5351 uptake and a correlation with language function in temporal GM but not in WM, which is consistent with a previous study reporting that svPPA-TDP primarily affected the GM [33]. In another $^{18}$F-THK5351 study in svPPA patients, $^{18}$F-THK5351 retention was elevated in the anteroinferior and lateral temporal cortices compared with that in the normal controls, and in the left inferior and temporal polar region compared with that in AD patients [34]. One potential explanation is the spill-out from off-target binding to the expression of MAO-B. However, patients with SD showed increased $^{18}$F-AV-1451 uptake—for which there is a paucity of evidence for binding to MAO-B—in the temporal lobe, which is the region primarily affected by TDP-43 and not tau pathology [35]. Another possibility is that $^{18}$F-THK5351 could bind to proteins associated with abnormal tau shown to coexist with TDP-43 [36].

In patients with bvFTD, the association between WM DTI and impaired social cognition was more consistent than the corresponding GM association [37]. Accelerated functional impairment early in the disease course in bvFTD can be explained by disruption of the salience connectivity network, dedicated to social-emotional functions [38]. The salience network has been reported to be related to WM pathology and spread of tau accumulation throughout the WM tract in the frontoinsular-cingulo-orbitofrontal network in bvFTD [39]. Therefore, during interpretation of $^{18}$F-THK5351 PET images, WM regions rather than GM regions are more useful in assessing cognitive function in patients with bvFTD.

A limitation of our study is the absence of postmortem confirmation of pathology. Based on our data, whether WM precedes or follows GM injury is unclear. Longitudinal analyses assessing the tandem evolution of WM and GM alterations are necessary. Furthermore, interpretation of the $^{18}$F-THK5351 PET may be confounded by MAO-B availability, as a substantial reduction in $^{18}$F-THK5351 binding has been observed after selegiline administration [13]. Increased uptake of $^{18}$F-AV-1451 has been shown in FTD as well as in AD [40, 41]. $^{18}$F-THK5351 can facilitate differentiation between FTD and non-FTD, because it has shown higher uptake in frontal WM compared with AD. However, according to a head-to-head comparison of $^{18}$F-THK5351 and $^{18}$F-AV-1451, $^{18}$F-THK5351 uptake was less prominent than $^{18}$F-AV-1451 uptake in AD [41], suggesting that $^{18}$F-THK5351 is less suitable than $^{18}$F-AV-1451 for evaluating AD [41]. In bvFTD patients, we observed higher WM/GM ratios than previously reported in a tau immunohistochemistry study [11]. This discrepancy suggests that combined tau and MAO-B binding in glial cells contributes to increased WM $^{18}$F-THK5351 uptake in bvFTD. Further studies with MAO-B inhibitor radioligands may clarify the percentages of $^{18}$F-THK5351 PET signal derived from MAO-B and tau binding in the frontal WM of patients with bvFTD.

## Conclusion

Frontal WM $^{18}$F-THK5351 uptake was higher in bvFTD than in other dementias, although there was no difference in GM uptake. The frontal WM uptake increased more prominently than GM uptake, and correlated well with executive function. These findings suggest that frontal WM changes reflect neuropathological differences between bvFTD and other dementias. Changes in WM rather than GM may have better utility in assessing cognitive function by $^{18}$F-THK5351 PET imaging in patients with bvFTD.

**Acknowledgments** This work was supported by a grant from the Korea Health Technology R&D Project through the Korea Health Industry Development Institute, funded by the Ministry of Health & Welfare, Republic of Korea (HI14C2768).

### Compliance with ethical standards

**Conflict of interest** The authors declare that they have no conflict of interest.

**Informed consent** Written informed consent was obtained from all individual participants included in the study.

**Ethics approval** All procedures performed in studies involving human participants were in accordance with the ethical standards of the institutional and/or national research committee and with the principles of the1964 Declaration of Helsinki and its later amendments or comparable ethical standards.

## References

1. Ballatore C, Lee VM, Trojanowski JQ. Tau-mediated neurodegeneration in Alzheimer's disease and related disorders. Nat Rev Neurosci. 2007;8:663–72. https://doi.org/10.1038/nrn2194.
2. Neary D, Snowden JS, Gustafson L, Passant U, Stuss D, Black S, et al. Frontotemporal lobar degeneration: a consensus on clinical diagnostic criteria. Neurology. 1998;51:1546–54.
3. Siri S, Benaglio I, Frigerio A, Binetti G, Cappa SF. A brief neuropsychological assessment for the differential diagnosis between frontotemporal dementia and Alzheimer's disease. Eur J Neurol. 2001;8:125–32.
4. Beach TG, Monsell SE, Phillips LE, Kukull W. Accuracy of the clinical diagnosis of Alzheimer disease at National Institute on Aging Alzheimer disease centers, 2005-2010. J Neuropathol Exp

Neurol. 2012;71:266–73. https://doi.org/10.1097/NEN.0b013e31824b211b.
5. Ossenkoppele R, Pijnenburg YA, Perry DC, Cohn-Sheehy BI, Scheltens NM, Vogel JW, et al. The behavioural/dysexecutive variant of Alzheimer's disease: clinical, neuroimaging and pathological features. Brain. 2015;138:2732–49. https://doi.org/10.1093/brain/awv191.
6. Rabinovici GD, Rosen HJ, Alkalay A, Kornak J, Furst AJ, Agarwal N, et al. Amyloid vs FDG-PET in the differential diagnosis of AD and FTLD. Neurology. 2011;77:2034–42. https://doi.org/10.1212/WNL.0b013e31823b9c5e.
7. Borroni B, Brambati SM, Agosti C, Gipponi S, Bellelli G, Gasparotti R, et al. Evidence of white matter changes on diffusion tensor imaging in frontotemporal dementia. Arch Neurol. 2007;64:246–51. https://doi.org/10.1001/archneur.64.2.246.
8. Taipa R, Brochado P, Robinson A, Reis I, Costa P, Mann DM, et al. Patterns of microglial cell activation in Alzheimer disease and frontotemporal lobar degeneration. Neurodegener Dis. 2017;17:145–54. https://doi.org/10.1159/000457127.
9. Heneka MT, Kummer MP, Latz E. Innate immune activation in neurodegenerative disease. Nat Rev Immunol. 2014;14:463–77. https://doi.org/10.1038/nri3705.
10. Leyns CEG, Holtzman DM. Glial contributions to neurodegeneration in tauopathies. Mol Neurodegener. 2017;12:50. https://doi.org/10.1186/s13024-017-0192-x.
11. Sander K, Lashley T, Gami P, Gendron T, Lythgoe MF, Rohrer JD, et al. Characterization of tau positron emission tomography tracer [(18)F]AV-1451 binding to postmortem tissue in Alzheimer's disease, primary tauopathies, and other dementias. Alzheimers Dement. 2016;12:1116–24. https://doi.org/10.1016/j.jalz.2016.01.003.
12. Harada R, Okamura N, Furumoto S, Furukawa K, Ishiki A, Tomita N, et al. 18F-THK5351: a novel PET radiotracer for imaging neurofibrillary pathology in Alzheimer disease. J Nucl Med. 2016;57:208–14. https://doi.org/10.2967/jnumed.115.164848.
13. Ng KP, Pascoal TA, Mathotaarachchi S, Therriault J, Kang MS, Shin M, et al. Monoamine oxidase B inhibitor, selegiline, reduces (18)F-THK5351 uptake in the human brain. Alzheimers Res Ther. 2017;9:25. https://doi.org/10.1186/s13195-017-0253-y.
14. Harada R, Ishiki A, Kai H, Sato N, Furukawa K, Furumoto S, et al. Correlations of (18)F-THK5351 PET with post-mortem burden of tau and astrogliosis in Alzheimer's disease. J Nucl Med. 2017. https://doi.org/10.2967/jnumed.117.197426.
15. Kang Y, Na DL, Hahn S. Seoul Neuropsychological Screening Battery. Incheon: Human Brain Research & Consulting Co.; 2003.
16. McKhann GM, Knopman DS, Chertkow H, Hyman BT, Jack CR, Kawas CH, et al. The diagnosis of dementia due to Alzheimer's disease: recommendations from the National Institute on Aging-Alzheimer's Association workgroups on diagnostic guidelines for Alzheimer's disease. Alzheimers Dement. 2011;7:263–9. https://doi.org/10.1016/j.jalz.2011.03.005.
17. Petersen RC, Smith GE, Waring SC, Ivnik RJ, Kokmen E, Tangelos EG. Aging, memory, and mild cognitive impairment. Int Psychogeriatr. 1997;9(Suppl 1):65–9.
18. Knopman DS, Kramer JH, Boeve BF, Caselli RJ, Graff-Radford NR, Mendez MF, et al. Development of methodology for conducting clinical trials in frontotemporal lobar degeneration. Brain. 2008;131:2957–68. https://doi.org/10.1093/brain/awn234.
19. Thomas BA, Erlandsson K, Modat M, Thurfjell L, Vandenberghe R, Ourselin S, et al. The importance of appropriate partial volume correction for PET quantification in Alzheimer's disease. Eur J Nucl Med Mol Imaging. 2011;38:1104–19. https://doi.org/10.1007/s00259-011-1745-9.
20. Ossenkoppele R, Schonhaut DR, Scholl M, Lockhart SN, Ayakta N, Baker SL, et al. Tau PET patterns mirror clinical and neuroanatomical variability in Alzheimer's disease. Brain. 2016;139:1551–67. https://doi.org/10.1093/brain/aww027.
21. Schofield E, Kersaitis C, Shepherd CE, Kril JJ, Halliday GM. Severity of gliosis in Pick's disease and frontotemporal lobar degeneration: tau-positive glia differentiate these disorders. Brain. 2003;126:827–40.
22. Shi J, Shaw CL, Du Plessis D, Richardson AM, Bailey KL, Julien C, et al. Histopathological changes underlying frontotemporal lobar degeneration with clinicopathological correlation. Acta Neuropathol. 2005;110:501–12. https://doi.org/10.1007/s00401-005-1079-4.
23. Serrano-Pozo A, Mielke ML, Gomez-Isla T, Betensky RA, Growdon JH, Frosch MP, et al. Reactive glia not only associates with plaques but also parallels tangles in Alzheimer's disease. Am J Pathol. 2011;179:1373–84. https://doi.org/10.1016/j.ajpath.2011.05.047.
24. Lu PH, Lee GJ, Shapira J, Jimenez E, Mather MJ, Thompson PM, et al. Regional differences in white matter breakdown between frontotemporal dementia and early-onset Alzheimer's disease. J Alzheimers Dis. 2014;39:261–9. https://doi.org/10.3233/JAD-131481.
25. Zhang Y, Schuff N, Du AT, Rosen HJ, Kramer JH, Gorno-Tempini ML, et al. White matter damage in frontotemporal dementia and Alzheimer's disease measured by diffusion MRI. Brain. 2009;132:2579–92. https://doi.org/10.1093/brain/awp071.
26. Hardy J, Revesz T. The spread of neurodegenerative disease. N Engl J Med. 2012;366:2126–8. https://doi.org/10.1056/NEJMcibr1202401.
27. Tartaglia MC, Zhang Y, Racine C, Laluz V, Neuhaus J, Chao L, et al. Executive dysfunction in frontotemporal dementia is related to abnormalities in frontal white matter tracts. J Neurol. 2012;259:1071–80. https://doi.org/10.1007/s00415-011-6300-x.
28. Avants BB, Cook PA, Ungar L, Gee JC, Grossman M. Dementia induces correlated reductions in white matter integrity and cortical thickness: a multivariate neuroimaging study with sparse canonical correlation analysis. NeuroImage. 2010;50:1004–16. https://doi.org/10.1016/j.neuroimage.2010.01.041.
29. Fowler JS, Volkow ND, Wang GJ, Logan J, Pappas N, Shea C, et al. Age-related increases in brain monoamine oxidase B in living healthy human subjects. Neurobiol Aging. 1997;18:431–5.
30. Hodges JR, Mitchell J, Dawson K, Spillantini MG, Xuereb JH, McMonagle P, et al. Semantic dementia: demography, familial factors and survival in a consecutive series of 100 cases. Brain. 2010;133:300–6. https://doi.org/10.1093/brain/awp248.
31. Spinelli EG, Mandelli ML, Miller ZA, Santos-Santos MA, Wilson SM, Agosta F, et al. Typical and atypical pathology in primary progressive aphasia variants. Ann Neurol. 2017;81:430–43. https://doi.org/10.1002/ana.24885.
32. Josephs KA, Hodges JR, Snowden JS, Mackenzie IR, Neumann M, Mann DM, et al. Neuropathological background of phenotypical variability in frontotemporal dementia. Acta Neuropathol. 2011;122:137–53. https://doi.org/10.1007/s00401-011-0839-6.
33. Brettschneider J, Del Tredici K, Irwin DJ, Grossman M, Robinson JL, Toledo JB, et al. Sequential distribution of pTDP-43 pathology in behavioral variant frontotemporal dementia (bvFTD). Acta Neuropathol. 2014;127:423–39. https://doi.org/10.1007/s00401-013-1238-y.
34. Lee H, Seo S, Lee SY, Jeong HJ, Woo SH, Lee KM, et al. [$^{18}$F]-THK5351 PET imaging in patients with semantic variant primary progressive aphasia. Alzheimer Dis Assoc Disord. 2018;32(1):62–9. https://doi.org/10.1097/wad.0000000000000216.
35. Bevan-Jones WR, Cope TE, Jones PS, Passamonti L, Hong YT, Fryer TD, et al. [(18)F]AV-1451 binding in vivo mirrors the expected distribution of TDP-43 pathology in the semantic variant of primary progressive aphasia. J Neurol Neurosurg Psychiatry. 2017. https://doi.org/10.1136/jnnp-2017-316402.

36. Cairns NJ, Bigio EH, Mackenzie IR, Neumann M, Lee VM, Hatanpaa KJ, et al. Neuropathologic diagnostic and nosologic criteria for frontotemporal lobar degeneration: consensus of the Consortium for Frontotemporal Lobar Degeneration. Acta Neuropathol. 2007;114:5–22. https://doi.org/10.1007/s00401-007-0237-2.
37. Downey LE, Mahoney CJ, Buckley AH, Golden HL, Henley SM, Schmitz N, et al. White matter tract signatures of impaired social cognition in frontotemporal lobar degeneration. Neuroimage Clin. 2015;8:640–51. https://doi.org/10.1016/j.nicl.2015.06.005.
38. Zhou J, Greicius MD, Gennatas ED, Growdon ME, Jang JY, Rabinovici GD, et al. Divergent network connectivity changes in behavioural variant frontotemporal dementia and Alzheimer's disease. Brain. 2010;133:1352–67.
39. Seeley WW, Menon V, Schatzberg AF, Keller J, Glover GH, Kenna H, et al. Dissociable intrinsic connectivity networks for salience processing and executive control. J Neurosci. 2007;27:2349–56. https://doi.org/10.1523/JNEUROSCI.5587-06.2007.
40. Spina S, Schonhaut DR, Boeve BF, Seeley WW, Ossenkoppele R, O'Neil JP, et al. Frontotemporal dementia with the V337M MAPT mutation: tau-PET and pathology correlations. Neurology. 2017;88(8):758–66. https://doi.org/10.1212/wnl.0000000000003636.
41. Jang YK, Lyoo CH, Park S, Oh SJ, Cho H, Oh M, et al. Head to head comparison of [$^{18}$F] AV-1451 and [$^{18}$F] THK5351 for tau imaging in Alzheimer's disease and frontotemporal dementia. Eur J Nucl Med Mol Imaging. 2018;45(3):432–42. https://doi.org/10.1007/s00259-017-3876-0.